Pergamon

PII: S0191-8141(97)00118-1

Journal of Structural Geology, Vol. 20, No. 4, pp. 473 to 486, 1998

0191-8141/98 $19.00 + 0.00

Incorporating spatial distribution into stochastic modelling of fractures: multifractals and Lévy-stable statistics

WILLIAM C. BELFIELD

Reservoir Research & Technical Services, ARCO Exploration & Production Technology, Plano, TX 75075, U.S.A.

(*Received* 9 *May* 1997; *accepted in revised form* 18 *December* 1997)

Abstract—A new approach to the stochastic modelling of fractures is developed using data acquired in horizontal wells and applied to one-dimensional simulations. It differs from previous studies in the use of both Lévy-stable statistics to describe the fracture attributes and of a (multifractal) strain-based model to create the spatial distribution. The structure of the multifractal strain is generated with a multiplicative cascade and used as a template or guide in the simulation. Resulting simulations have scale-invariant structure. Spacing distribution functions depend on the spatial partitioning of strain. For the case where strain distribution is homogeneous an approximate negative exponential spacing distribution results. Heterogeneous strain, exhibiting intermittency, leads to power-law (fractal) spacing distributions and spatial clustering. When plotting spacing as log–log cumulative frequency, the slope (fractal dimension) quantifies the degree of clustering. Small fractal dimensions are indicative of more clustering than large ones, the degree of clustering decreasing with an increase in fractal dimension. © 1998 Elsevier Science Ltd. All rights reserved

INTRODUCTION

The characterisation of joints and subseismic faults, known to exist in the interwell region, remains an unresolved problem. Examination of data from different scales is common in attempting to evaluate the distribution and significance of joints or faults in reservoirs. Core and wireline logs can sample either type of discontinuity, but they access an extremely small reservoir volume. Seismic imaging can resolve large displacement faults, yet fails to delineate small-scale brittle features. Engineering information from pressure transient or tracer tests provide a response from the interwell scale, but one that averages over the flow properties of a fracture network and does not constrain its geometry. One approach for estimating the distribution of structural heterogeneity in the interwell region is stochastic modelling. In this process, it is necessary to characterise statistically the attributes (length, displacement, aperture, spacing, orientation) associated with faults or joints and their spatial distribution (Gauthier and Lake, 1993).

Observations indicate that it is possible to describe fracture attributes with a variety of statistical distributions. Joint length and aperture are often interpreted to follow a log-normal distribution (Long and Billaux, 1987). More recently, numerous studies (Childs *et al.*, 1990; Heffer and Bevan, 1990; Marrett and Allmendinger, 1991), covering a range of scale from outcrop to seismic, suggest that fault systems have attributes that follow a power-law or fractal distribution. These distributions offer the enticing potential of using observations at some large scale to estimate statistical characteristics at some smaller scale.

In contrast to the characterisation and analysis of attribute distributions, spatial distribution of fracture systems has been less successful. In particular, there is no technique for incorporating scale-invariant behaviour into the spatial arrangement of stochastic faults or joints. Poisson models of spatial distribution consider that fractures are independent and lack spatial correlation. As such, they necessarily lead to negative exponential spacing distributions and fail to account for the clustering of joints (Laubach, 1991) or faults (Gillespie *et al.*, 1993) often observed in outcrop. Examples of negative exponential spacing in fault systems are rare (Brooks *et al.*, 1996). Other reports indicate that joint spacing is often log-normal (Narr and Suppe, 1991) or fractal (Belfield and Sovich, 1995). Log-normal or fractal spacing statistics indicate that fractures are not distributed independently. Despite this, the process of randomly placing objects and assigning attributes chosen from a defined statistical distribution has been used extensively to model fractures in hydrologic systems (Long *et al.*, 1982; Cacas *et al.*, 1990; Chilès and de Marsily, 1993). Similar marked point processes have been used to define the size and spatial distribution of subseismic faults, treating them as random objects (Munthe *et al.*, 1993; Godderij *et al.*, 1995). Parent/daughter models (Hestir *et al.*, 1987) distribute the parents (e.g. larger scale faults) at random and then cluster smaller ones (daughters) around them.

Early attempts at assessing the scale-invariant nature of fracture spatial distribution involved box-counting on outcrops (Barton and Larson, 1985). When the number of boxes containing a fracture segment was plotted against box size on log–log coordinates, a non-integer slope was found, indicating fractal behaviour.

However, other outcrop studies found either that fracture spatial distribution was characterised by a log–log straight line having an integer slope (Odling, 1992) or a distribution that could not be described by a single log–log straight line (Chilès, 1988). Additional studies on both faults and joints have found a similar inability of single straight log–log lines to describe the spatial distribution (Walsh and Watterson, 1993; Gillespie *et al.*, 1993). Furthermore, it seems reasonable to assume that strain magnitude and distribution will play a major role in dictating the spatial statistics (Wu *et al.*, 1995; Becker and Gross, 1996) of these systems.

The present study examines an alternative approach to the stochastic modelling of fractures. It differs from previous studies in the use of both Lévy-stable statistics to describe the attributes of fracture systems and a (multifractal) strain-based model to create the spatial distribution. Unlike other methods that treat attributes and spatial distribution independently, multifractals provide a scale-invariant coupling of physical characteristic to spatial distribution. The ability to incorporate both spatial clustering and scaling in stochastic simulations has led to their increasing use in the geophysical sciences (Main, 1996). The basic approach is to generate a strain distribution using a multiplicative cascade where random multipliers are chosen from a Lévy-stable distribution. This spatial strain distribution can be thought of as a template upon which stochastic fractures with assigned displacements or apertures are distributed. Spatial distribution of the fractures is constrained by the allocated strain. Simulations using different spatial distributions of strain, ranging from homogeneous to heterogeneous, lead to distinct spacing statistics. It is possible to quantify the degree of clustering from the resulting spacing distribution functions.

It is important to emphasise two factors relating to the data that form the basis of the analysis here. One, is that the data come from horizontal wells and, as such, both the data and simulations are one-dimensional. Second, the fractures that comprise the data are probably joints with some possible small displacement faults. I use the term fracture in a generic context, treating faults and joints as analogous in a geometric sense. As such, the approach is completely general and should be applicable to either discontinuity. However, studies on additional fault and joint datasets will be necessary to verify this view.

The paper begins with a discussion of Lévy-stable distributions and the relationship of multifractals to strain. An introduction to the modelling of (multifractal) strain distributions using multiplicative cascades follows. Then, three example stochastic simulations with different strain models are used to illustrate fracture spatial clustering. Finally, a multiplicative cascade is used to generate a strain distribution based on information from a horizontal well. Simulation of stochastic fractures on this cascade is shown to have spacing characteristics similar to those found in the well.

SCALING DISTRIBUTIONS

Scaling means that an object looks the same regardless of its size. Conversely, an object whose true size cannot be determined by visual examination is said to have scaling properties. Many geological objects exhibit scaling characteristics and require some measure of scale when photographing or otherwise depicting them. Without a scale bar it is difficult to definitively identify the size of the object.

The geometric similarity between fault arrays occurring at different scales has been recognised for some time (Tchalenko, 1970). This similarity reflects the mechanical processes that operate at all scales. Mandelbrot (1982) points out that scaling must be defined independent of geometry. In this sense, scaling refers to identical statistical distributions that differ only by a scale factor. Lévy-stable distributions satisfy this necessary condition for scaling (Feller, 1971). These distributions have power-law tails where for large l, the probability of encountering a size $L > l$ is $\Pr(L > l) \sim l^{-\alpha}$ with $0 < \alpha < 2$.

Symmetric Lévy distributions have probability density

$$p(x) = \pi^{-1} \int_0^\infty \exp[-(Ck)^\alpha] \cos(kx)\, \mathrm{d}k \qquad (1)$$

characterised by two parameters, the Lévy index, α, lying in the range $0 < \alpha \leq 2$, and C, a parameter that describes the width of the distribution (Painter *et al.*, 1995). When $\alpha = 2$ the Lévy probability density is equivalent to a Gaussian distribution. Small α values correspond to broader distributions with longer tails and more extreme values. Samples from the extreme parts of the tails can lead to physically unrealistic values when attempting to fit Lévy distributions to real data. Such random samples of Lévy distributions can extend beyond the range of the empirical data requiring truncation of the sample distribution in order to fit the data (Mantegna and Stanley, 1995). Random sampling of symmetric Lévy distributions (Mantegna, 1994) with zero mean is used throughout the paper. These values are taken to be logarithmic and must be exponentiated prior to comparison with empirical data.

Most empirical data interpreted to be fractal will contain values that deviate from strict power-law behaviour in the range of smaller-size values of the particular dataset. When plotting log cumulative frequency vs log size, the deviation is manifest as a flattening of the curve so that the data distribution resembles an inverted hockey stick. This flattening is usually taken to be an artefact of resolution or bias (Heffer and

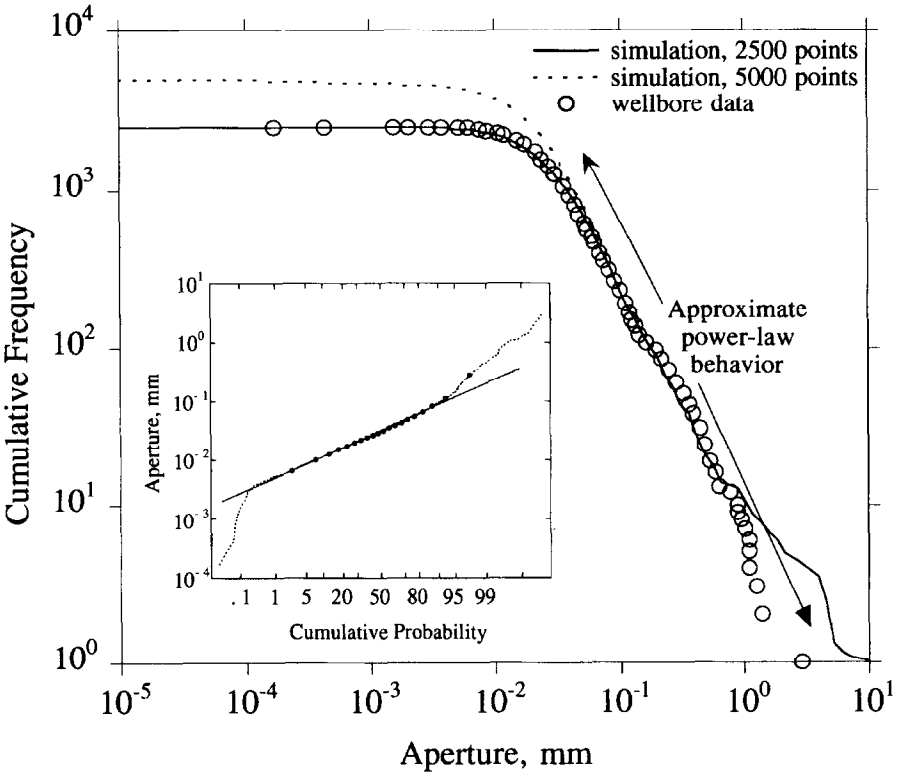

Fig. 1. Lévy-stable fit to an experimental dataset. Fracture apertures (circles) from measurements along a horizontal wellbore fit with a Lévy-stable distribution (solid line) with $\alpha = 1.85$ and $C = 0.66$. Hypothetical distribution for 5000 apertures (dashed line) and similar Lévy parameters. The dashed distribution follows that of the solid one to an aperture of 0.06 mm at which point it continues along the straight log–log trend as the solid line begins to deviate. The inability of the wellbore data to extend to the smaller apertures of the projected solid line fit reflect resolution limits of the wellbore data collection. Inset shows wellbore data plotted as cumulative probability. Note that 90% of the data conform quite well to a log-normal distribution. Just the (large aperture) tail deviates, consistent with Lévy-stable behaviour.

Bevan, 1990; Watterson *et al.*, 1996). Although resolution dependency is a factor to some degree, the proposal made here is that the deviation is a reflection of random sampling from an underlying Lévy-stable probability distribution. Because Lévy-stable distributions asymptotically approach power-law behaviour they are able to account for both the empirical data points that follow power-law behaviour and those that deviate from it. To illustrate this, consider an empirical fracture aperture dataset, collected along a horizontal wellbore with an electrical imaging tool, that follows approximate power-law behaviour for almost two orders of magnitude (Fig. 1). Deviation of the data from this behaviour occurs approximately at an aperture of 0.05 mm. Smaller values below this point account for 80% of the data. By random sampling of a Lévy distribution with $\alpha = 1.85$ and $C = 0.66$ it is possible to fit 99% of the data (Fig. 1; solid line). If it were possible to double the number of samples, for example, by having an imaging tool that covers a larger percentage of the borehole, then a similar-shaped distribution enlarged on both axes will result (Fig. 1; dashed line). Some datasets, when examined over a large range of different scales, exhibit a deviation from power-law behaviour as evidenced by a flattening of data on the log–log plots *at all scales* (Castaing *et al.*, 1996; Odling, 1997). In some cases, it is hard to explain this deviation as being a function of resolution because data sampling is intensive and the area of observation is small (Schlische *et al.*, 1996; Knott *et al.*, 1996). The evidence cited here suggests that the statistical character of fracture attribute empirical data is fully consistent with Lévy-stable distributions.

One final aspect of Lévy-stable distributions can be illustrated by plotting the aperture data as cumulative probability (Fig. 1; inset) instead of on log–log axes. It can be seen that approximately 90% of the data closely fits a log-normal distribution. Deviation from log-normality occurs in the tails. At very small apertures the deviation reflects limited resolution, but large values characterise the high end (power-law) tail of the Lévy distribution. Interpreting such data as log-normal, despite the deviation in the large value tail, is common (e.g. Einstein and Baecher, 1983). I will return to a further comparison of log-normal and Lévy distributions later in the paper. It should be clear that random sampling of Lévy-stable distributions is capable of creating cumulative distributions that have power-law character and account for empirical observations of samples deviating from strict power-law behaviour. Furthermore, additional sampling of the same distribution leads to self-similar scaling beha-

viour. By varying the parameters α and C, distributions with a range of power-law slopes are possible. This flexibility is used below to create widely different multifractal distributions.

INCORPORATING SPATIAL DISTRIBUTION INTO STOCHASTIC MODELS

Stochastic models and fracture spatial distribution

Rives *et al.* (1992) studied the evolution of joint spacing in both analogue and simulation models. One observation was that joint spacing evolves from a negative exponential distribution to a log-normal form and finally to a normal distribution with increasing strain. They do not give any indication of encountering fractal or power-law spacing in their models. Reasoning that at low strains joints can grow more-or-less independent of each other, it was suggested that initial joint spacing is governed by a random process. With increasing strain the joints interact and become organised leading to different spacing characteristics. Numerical simulations of a growing fault population (Cowie *et al.*, 1995) show a similar organisation with increasing strain.

In modelling the interaction process, Rives *et al.* (1992) add joints randomly along a line trace, but reject them if they land too close to an existing joint. This was taken to be an analogue of the stress shadowing that large joints impose upon a zone surrounding the joint (Pollard and Segall, 1987). Rives *et al.* (1992) regard, consistent with their experimental models, that spacing evolution depends on the *magnitude* of strain. As a modelling device, the approach taken here suggests it is the *spatial distribution* of the strain, rather than the magnitude, that governs the spacing distribution. For brittle deformation, joint apertures and fault displacements determine the magnitude of strain. In general, this value exhibits a dependency on resolution (Gross and Engelder, 1995).

Multifractals and brittle strain distribution

Knowledge of a power-law cumulative frequency relationship for joint apertures or fault displacements tells nothing about their spatial distribution. Similarly, box-counting just indicates presence or absence of a fracture in a cell without any information about attribute magnitude. Characterisation with multifractals represents a coupling of these parameters by relating an attribute (e.g. aperture, displacement, length, etc.) to its spatial distribution. This transpires by the partitioning of measures into subsets and studying the scaling nature of the distributions for each subset (Evertsz and Mandelbrot, 1992; Davis *et al.*, 1994).

Brittle strain, resulting from the application of stress at shallow crustal conditions, is manifest as fractures at all scales. Belfield (1994) showed that apertures measured along a horizontal wellbore can be described by multifractal statistics. These apertures represent the extensional strain distribution of open fractures along the one-dimensional trace of the wellbore through the reservoir. This observation implies that the strain distribution, over the finite-resolution scale of the measuring device, is also multifractal.

Partitioning a measure along a wellbore is done by subdividing the well length into cells of equal size in the same way that box-counting is performed. For apertures along a horizontal wellbore, a normalised measure, λ_i is defined by

$$\lambda_i = p_i / \Sigma p_i \tag{2}$$

where p_i corresponds to the sum of apertures contained in a single cell and the summation is over all cells (Belfield, 1994). Defining the elongation, e, perpendicular to the fracture trend as

$$e = \Delta l / l_0 \tag{3}$$

where l_0 is the original interval length (taken to be unity) and Δl corresponds to the length change resulting from the introduction of extension fractures as measured by their apertures. Thus, (3) can be written as

$$e = \Delta l = \Sigma \mu_i \tag{4}$$

where the summation is over all individual fracture apertures, μ_i. The fractional elongation, ε_i, for i fractures is then

$$\varepsilon_i = \mu_i / \Sigma \mu_i \tag{5}$$

Thus, equations (2) and (5) have the same form indicating that the measure defined in equation (2) is the fractional elongation for a fractured interval.

Modelling strain distribution with multiplicative cascades

Processes with complex interactions over many scales often leave signatures that have multifractal characteristics. One phenomenological approach to represent these characteristics is with multiplicative cascades. These multifractal signatures are defined by measures that increase in variability with a decrease in the scale size. Conceptually, one can imagine being able to observe only large displacement faults at a coarse resolution, but as the scale of observation decreases (increasing resolution), smaller faults become apparent leading to greater variability. At each level of improving resolution the increasing variability is manifest in the widening of the displacement statistical distribution as smaller and smaller values are observed. In the cascade model, the increase in variability is introduced over the different scales by multiplication.

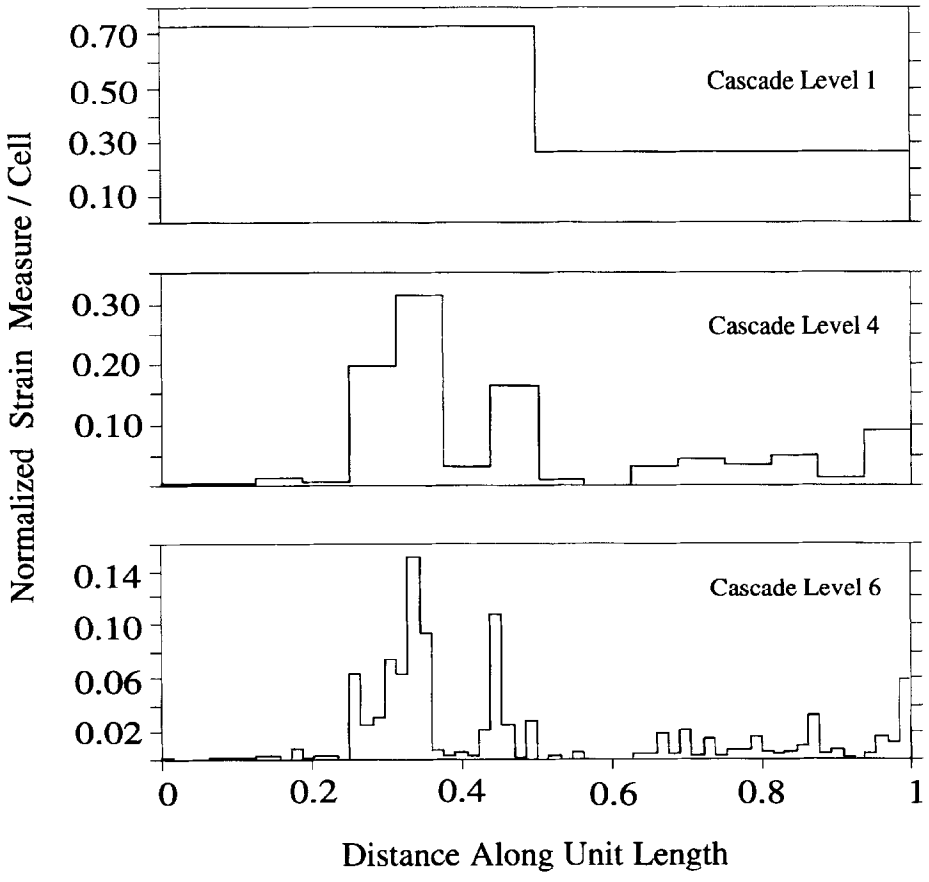

Fig. 2. Multiplicative strain cascade illustrated at three different levels. As the cascade proceeds a unit strain is continuously partitioned at each level. At the first level the unit interval is divided in half and the bulk of the strain is partitioned between 0 and 0.5. At level 4 the unit interval is divided into 16 cells with the largest strains residing from 0.2 to 0.4 and from 0.4 to 0.5. The strain distribution continues to be refined with additional cascades.

A simple 1-D multiplicative cascade model for strain distribution starts with a strain, P_0, on a line of unit length. Normalise the strain so that $P_0 = 1$. Two non-negative random values, P and P', are drawn from a unit mean distribution, ensuring that $P \neq P'$. For the first level, subdivide the unit line into two equal parts. Redistribute the strain, P_0, on each segment of the bisected unit line such that one segment has strain $P_0{*}P$ and the other segment has strain $P_0{*}P'$. Take the redistributed strains and normalise them so that $(P_0{*}P) + (P_0{*}P') = 1$. This procedure of bisection and strain redistribution continues for n ($n = 1,2,3,\ldots$) levels of subdivision. An example of subdivision and redistribution is shown in Fig. 2 for several different levels. At any level of subdivision, n, the line is divided into 2^n segments. Random values necessary to redistribute strain at all levels are chosen from a single Lévy distribution. The multiplicative process can be thought of as an improvement in resolution. Strain measured with a low degree of fidelity (e.g. at level 1) is broadly distributed. As resolution is increased (level > 1) the partitioning of strain becomes clearer (Fig. 2).

To illustrate how cascades reflect the input parameters and, ultimately, affect the spatial distribution of fractures, three cascades with divergent characteristics are created. In one model, a Lévy-stable distribution with $\alpha = 1.98$ and $C = 0.22$ is used to redistribute strain at each level of the cascade. These values lead to a homogeneous strain/cell spatial distribution because the large value of α and the small value of C mean that the variance of the random values chosen for the cascade will be small. In turn, this means that differences among strain/cell magnitudes at any level of subdivision will also be small. The second cascade also uses a Lévy-stable distribution to reapportion strain, but one that leads to a heterogeneous strain/cell spatial distribution. The heterogeneous strain cascade has Lévy parameters $\alpha = 1.85$ and $C = 0.66$. The third model is intermediate to the other two and generated using a Lévy distribution with $\alpha = 1.9$ and $C = 0.4$.

Each cascade continues for nine levels, resulting in 512 cells for the final step. Differences between heterogeneous and homogeneous cascades are significant (Fig. 3). Maximum and minimum strain/cell values in the homogeneous cascade differ by less than a factor of 10. In the heterogeneous cascade strain/cell values vary over eight orders of magnitude. Approximately 8% of the strain/cell values in the heterogeneous cascade are larger than the largest magnitude strain/cell

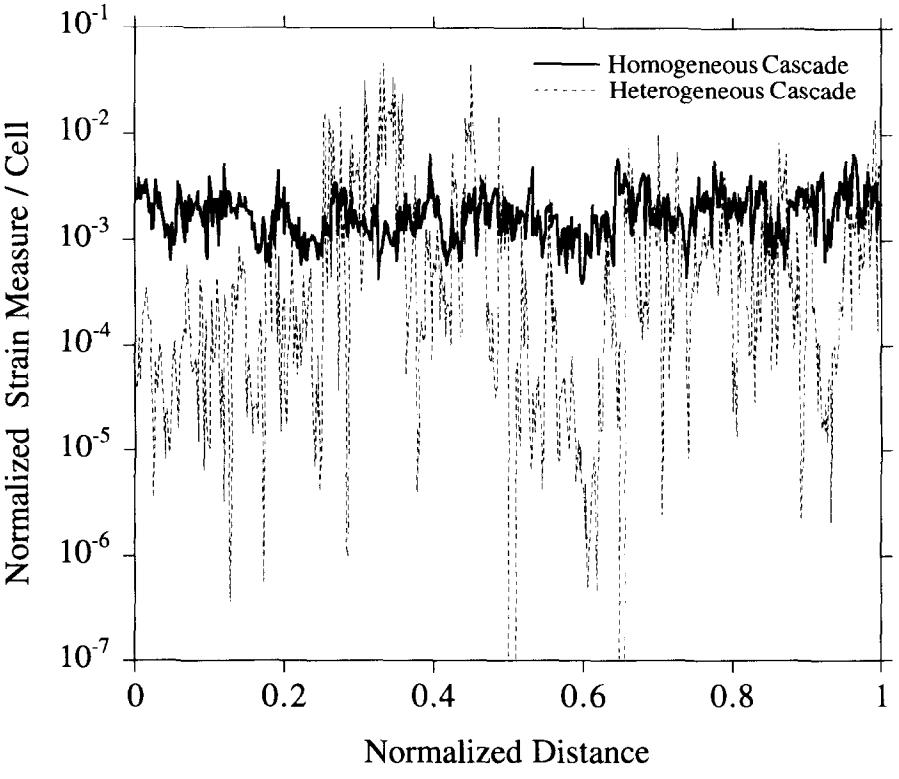

Fig. 3. Results for homogeneous and heterogeneous cascades after nine levels. The homogeneous cascades (solid line) result in minimum variability in strain measures/cell. Just the opposite is found for the heterogeneous cascade (dotted line) which has a high degree of variability in strain measures.

of the homogeneous cascade. Conversely, 56% of the heterogeneous strain/cell values are smaller than the smallest strain/cell value in the homogeneous cascade. In general, the heterogeneous cascade can be described as intermittent, with very large strain concentrations interspersed with areas of very low strain.

Simulation of discrete fractures on multiplicative strain cascades

The three multiplicative cascade examples are used to illustrate the stochastic modelling technique and the resulting differences in fracture spacing. The simulations are one-dimensional (as are the cascades) and can be thought of as representing a scan line through some reservoir interval. The basic approach is to add a fracture, of given aperture, to a cell along the modelled strain measure distribution where it will 'fit'. For an aperture to fit in a cell, the aperture must be smaller than the strain measure in the cell. For these examples, fracture apertures are chosen from a Lévy-stable distribution with $\alpha = 1.85$ and $C = 0.66$ (Fig. 1). For compatibility with the strain distribution, the apertures, μ_i, associated with the simulated fractures are normalised such that $\Sigma\mu_i = 1$ ($i = 1,2,3,\ldots,m$) where m corresponds to the number of fractures being simulated. All of the fracture simulations in this section use the same aperture distribution, so that the contrast in cascades is the sole variable. Resulting variation in spacing distribution is, therefore, a function only of differences in the spatial distribution of strain/cell.

Each simulation begins with the largest aperture and continues in descending aperture size order. Every cell in the highest order level (here 9 levels, 512 cells) cascade is tested to see if the strain measure in the cell exceeds that of the fracture aperture. Three possibilities exist: (1) the aperture is larger than the measure value in every cell at this level, (2) the aperture exceeds the measure value in all cells except one, (3) the aperture 'fits' in multiple cells. In the first case, cells in the next smallest level (level $n - 1$, where n is the present level) are then tested. The procedure continues to smaller levels until a cell value is found that exceeds the aperture value. For the second possibility, if the aperture fits in a single cell at the level, then the fracture is located randomly within this cell. In the case of multiple cells having measures that (at a single cascade level) exceed the aperture value, one of the cells is chosen at random and the fracture placed within that cell. Once a fracture is placed in a cell, the strain measure in the cell is reduced by the aperture magnitude prior to adding the next fracture.

There is a trade-off between the number of cascade levels and the accuracy in placing a fracture. A greater number of cascades requires more computer storage and search time testing strain measure values in cells. If, however, the cell sizes are too large, then the spacings begin to reflect the randomness of locations

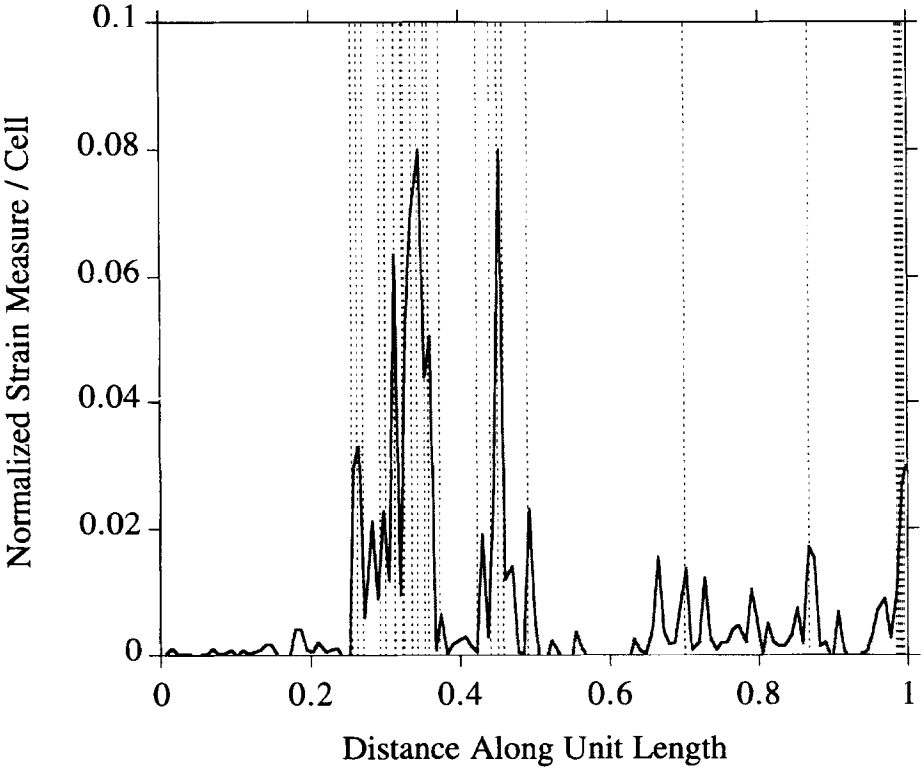

Fig. 4. Locations of 50 simulated fractures (dotted lines) on heterogeneous cascade. For clarity strain measures/cell (solid line) are shown for only 128 cells. Fractures are clustered on the cells containing the largest strain measures. Different realisations yield very similar results.

within cells. In the limit of only one cell (i.e. all fractures placed randomly), this reduces the spacing distribution to a Poisson model. Because the fractures are placed at random within cells, spacings smaller than the smallest cell size should be viewed with caution.

Results for different cascades

As an initial comparison, the location of 50 simulated fractures (Fig. 4; dotted line) are plotted on the unit line and compared to the heterogeneous strain measures (Fig. 4; solid line) when the entire interval is divided into 128 cells. There is a strong correlation between the fracture locations and the maximums in the strain/cell values. Clustering among the fractures is a result of the sparse occurrence of large strain/cell values along the interval. Intermittency of the large values is necessary for clustering to occur. Additional realisations will lead to minor differences in the location of the fractures, but, in general, the picture will not change significantly.

A set of 50 fractures were also simulated on the homogeneous strain cascade (Fig. 5). The distribution of fractures in this cascade is quite different than for the heterogeneous cascade. Here, the fractures are distributed more evenly (almost periodic) over the interval. There is little correspondence between maximum strain/cell values and the presence of a fracture. At some sites the fractures actually coincide with the troughs. Another realisation with this cascade could result in significantly different fracture locations, but not in the spacing distribution.

Other sets of simulations were run for each of the three cascades using 250 and 500 fractures with the intent of comparing fracture spacing characteristics. Distance between adjacent fractures was measured for all simulated fractures and tabulated in log–log cumulative frequency plots. For both the heterogeneous cascade and the intermediate cascade, fracture spacing distribution is found to have a log–log linear portion corresponding to a power-law or fractal distribution (Fig. 6). For the heterogeneous cascade this relationship continues for less than two orders of magnitude and has a slope (fractal dimension) of ~1.2. The intermediate cascade has a slope of about ~2.1, steeper than that of the heterogeneous cascade. At small spacing values both curves flatten as is typically seen in field data. The fractal dimension for fracture spacing was similar for both 250 and 500 fracture simulations in each of the two cascades. A different distribution function was found to describe the spacing characteristics from fracture simulations on the homogeneous cascade. This simulation yields a spacing distribution that plots close to negative exponential (Fig. 7). Attempts to fit a log–log slope to less than 100 points of this distribution produces a value of ~4.

Differences in the characteristics of the spacing distributions are a direct consequence of the spatial distri-

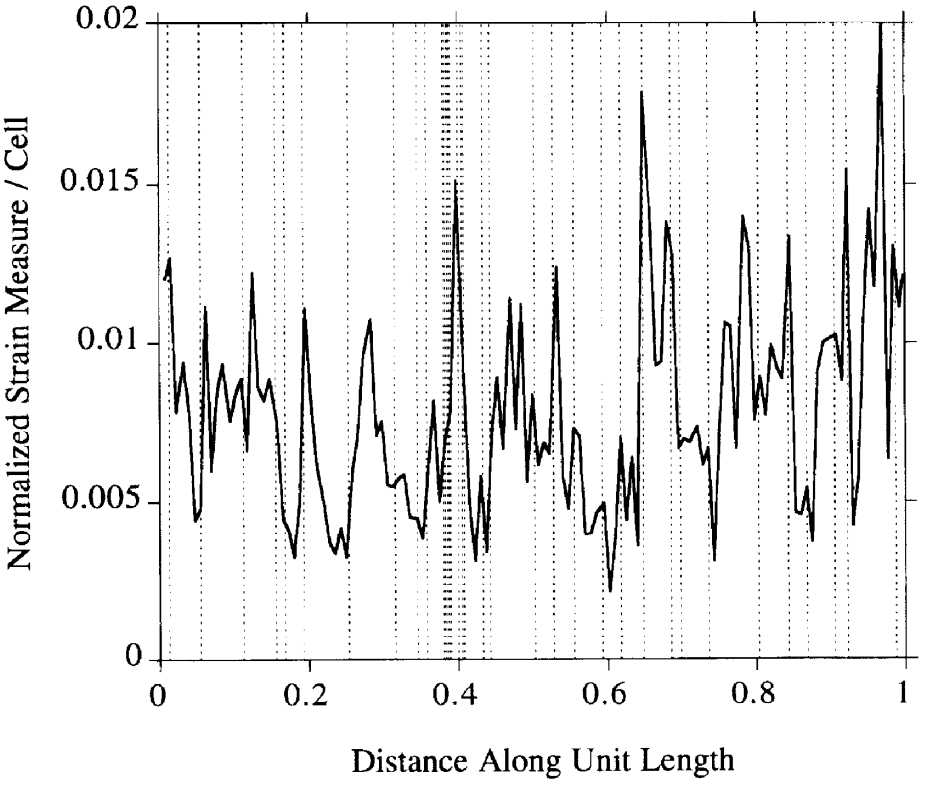

Fig. 5. Locations of 50 simulated fractures (dotted lines) on homogeneous cascade. For clarity strain measures/cell (solid line) are shown for only 128 cells. Unlike the heterogeneous cascade fractures here are evenly distributed. The small differences between strain measure/cell magnitudes result in some fractures being located in valleys between peaks.

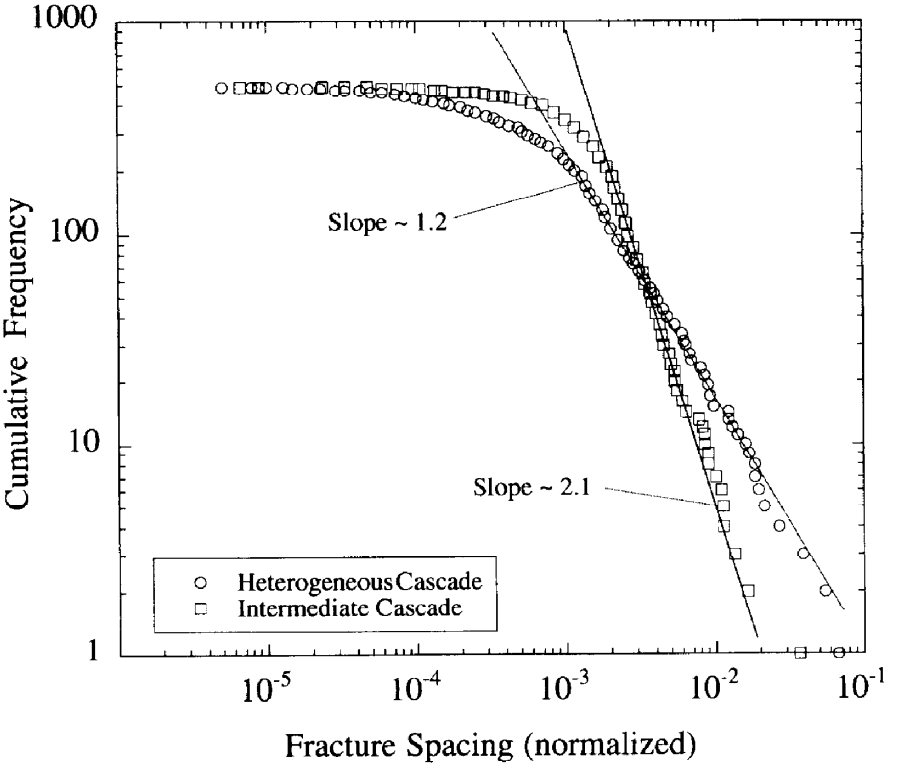

Fig. 6. Spacing distribution functions for 500 simulated fractures using heterogeneous and intermediate cascades. Both distributions have power-law slopes and flattening of the slopes at smaller spacing values, characteristics often found in natural examples. The heterogeneous cascade leads to a smaller spacing slope reflecting more fracture clustering than is found for the fracture distribution from the intermediate cascade.

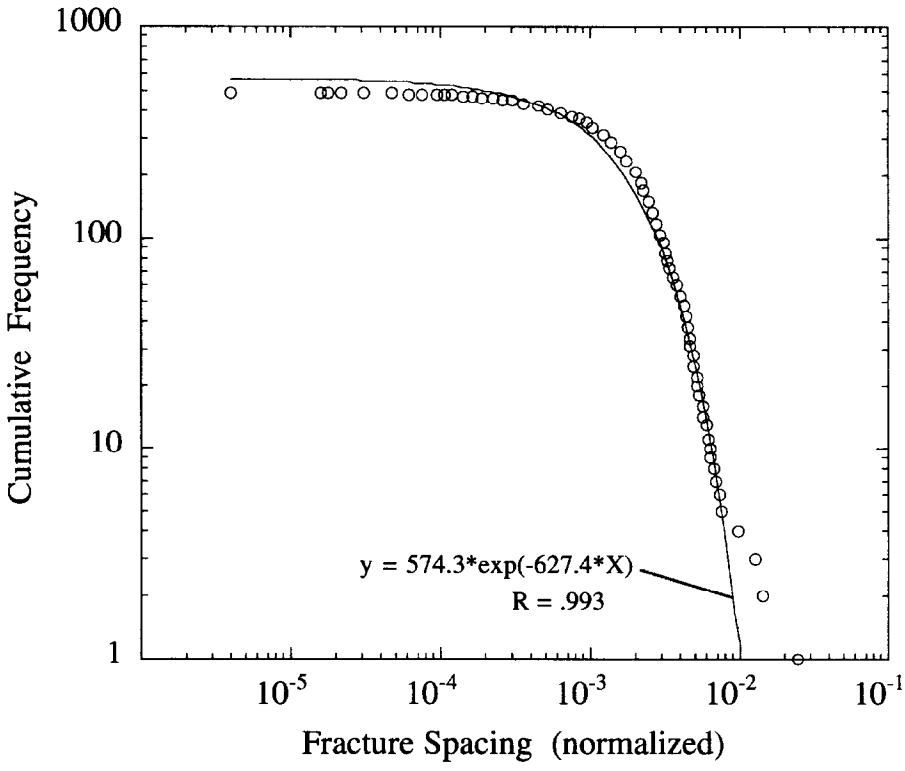

Fig. 7. Spacing distribution functions for 500 simulated fractures using the homogeneous cascade. The resulting distribution function is close to negative exponential. The steep part of the curve reflects the similar distance (almost periodic) between adjacent fractures.

bution of strain/cell in each cascade. In the homogeneous cascade, where little difference exists among strain/cell values, there is no strong preference for locating the fracture apertures being simulated in any particular cell on the grid. In a situation where the strain/cell values are uniform (i.e. no difference among values) placement of fractures is random and leads to a negative exponential spacing distribution. With the small differences found in the homogeneous cascade there are weak preferred locations resulting in an approximate negative exponential spacing distribution. As the strain/cell values become increasingly intermittent, approaching the partitioning of the heterogeneous cascade, spacing distribution becomes broader with small spacings reflecting fracture clustering and large spacings reflecting intercluster intervals. Characteristic of this broadening distribution is the power-law relationship apparent for the large spacings (Fig. 6). As discussed later in this paper, the log–log slope of this line is directly related to the clustering or intermittency of the strain/cell distribution.

Comparison to well data

The previous section dealt with the simulation of fractures for hypothetical strain/cell spatial distributions. As a further test of the simulation technique, a multiplicative cascade is created that is consistent with strain/cell values using fracture apertures from an actual well. Fractures are simulated along a line and the spacings compared with those measured from the well. The well data are from one of several horizontal wells that intersect a fracture system in a carbonate reservoir (Belfield and Sovich, 1995).

Generation of the strain/cell measures was done with a multiplicative cascade using a Lévy distribution with $\alpha = 1.9$ and $C = 0.3$, values similar to the intermediate model from the previous section. The Lévy parameters were determined by first dividing the wellbore into 512 equal size cells and tabulating normalised aperture measures in each (Belfield, 1994). Then testing sets of parameters through nine levels of cascade until finding a distribution of strain measures that compare favourably to the distribution of strain/cell measures from the actual well data (Fig. 8). Because 2500 fractures were measured in the horizontal well and simulating a similar number is necessary for comparison, the strain measure cascade was extended for another two levels creating 2048 cells. With this cascade (Fig. 9) there is a difference of four orders of magnitude between the smallest strain/cell values and the largest.

On this template of 2048 cells, 2500 fractures were simulated and the distance between adjacent fractures measured. The resulting spacing values show reasonable agreement with those of the actual data (Fig. 10). The underestimate of intermediate spacings around 10^{-4} (Fig. 10) of the simulation may reflect two fac-

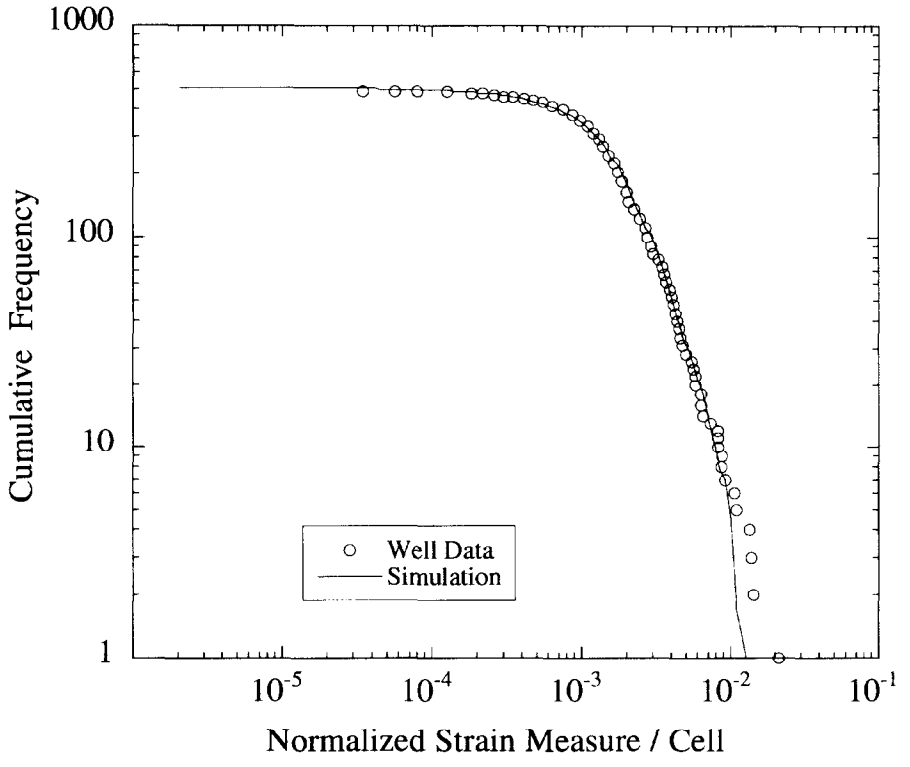

Fig. 8. Normalised strain measures (circles) were created from horizontal well fracture aperture data using 512 cells. Data were fit with a nine level multiplicative cascade using random numbers from a Lévy-stable distribution (α = 1.9, C = 0.3). The data are approximately log-normal.

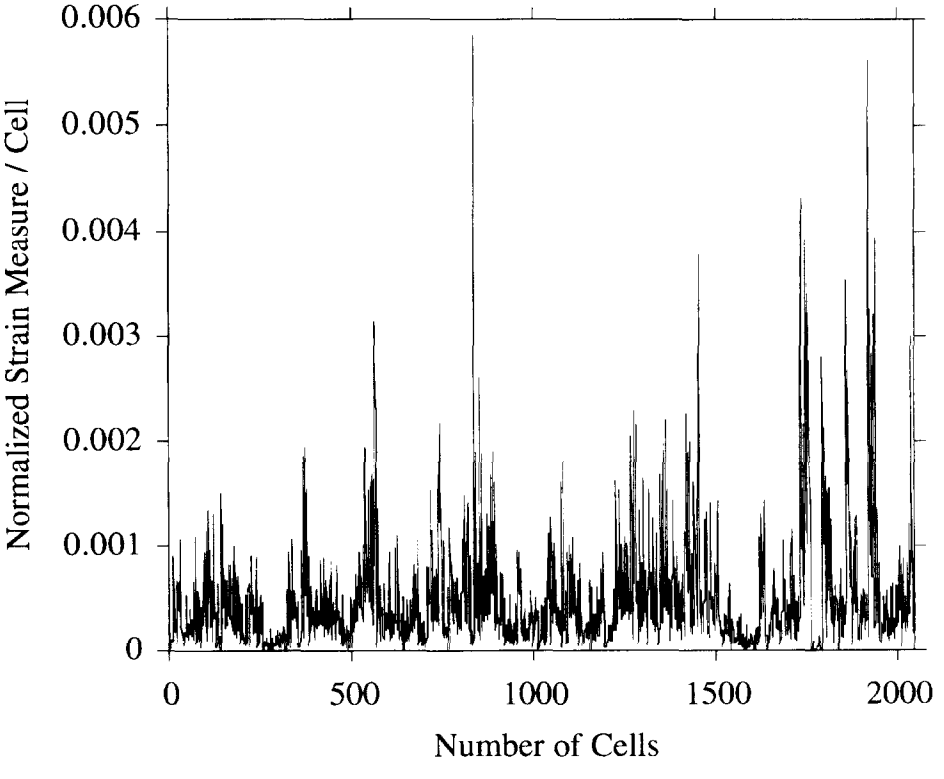

Fig. 9. Spatial distribution of simulated strain measures/cell for 2048 cells on a unit interval. The distribution is the result of expanding the cascade in Fig. 7 by another two levels. This spatial distribution and strain measure/cell magnitudes resemble that of the intermediate cascade discussed above.

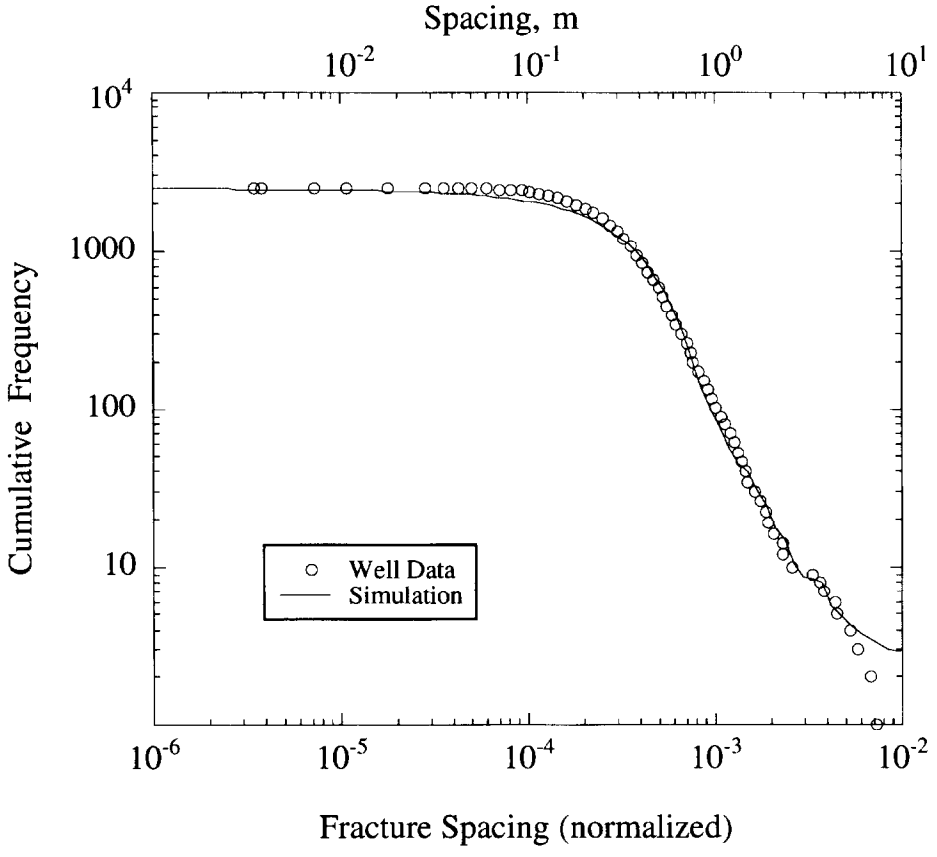

Fig. 10. Comparison between spacing of fractures from horizontal well (circles) and simulated fractures (solid line). Although the fit for 2500 fractures appears reasonable it can probably be improved by extending the cascade by another one or two levels.

tors. One is the potential for an insufficient number of cells in the cascade. Because the simulation locates fractures at random within a cell, more than one fracture per cell will result in a greater number of small spacings and a concomitant decrease in intermediate spacings. The other factor is that all random multipliers have been chosen from a single distribution. In effect, this makes each level of the cascade self-similar. This may be inconsistent with real data where self-affinity may be more appropriate (Jackson and Sanderson, 1992). However, because no special attempt was made to very accurately match the 512 cell cascade to the well data and because another two levels of cascade were added on, the fit is considered satisfactory.

CLUSTERING AND LOG-NORMAL DISTRIBUTIONS

The simulations demonstrate that it is possible to generate clustering based on strain spatial distributions. Contrary to expectations (Gillespie *et al.*, 1993; Nicol *et al.*, 1996), the ability to characterise clustering by parameters other than box-dimension (Barton, 1995) has been available, but unrealised. The degree of clustering is quantifiable using the slope (fractal dimension) of spacing vs cumulative frequency on a log–log plot (e.g. Fig. 6). Small (absolute) values of the slope indicate a high degree of clustering as strain spatial distribution becomes more intermittent. As the amount of clustering decreases, the value of the fractal dimension will increase. If the slope is steep (perhaps approaching a negative exponential fit) then the underlying strain distribution is relatively homogeneous indicating a lack of clustering. Generation of a multiplicative cascade produces a scale-invariant strain measure spatial distribution. With the multipliers being chosen from a single Lévy distribution, any interval (at one level) will resemble the whole distribution at any other level. Thus, the spacing distribution function will have the same character at all scales. For spacing this means that power-law distributions will occur at all scales and the slopes will be approximately the same.

Modelling of stochastic fractures using a template of spatially distributed strain measures leads to various distributions of fracture spacings. Missing from these spacing distributions is any mention of a log-normal distribution. Having shown earlier (Fig. 1) that a Lévy-stable and log-normal distributions bear a close resemblance even when $\alpha < 2$, I now show that log-normal distributions (i.e. Lévy-stable distributions with $\alpha = 2$) having sufficiently large dispersion can resemble

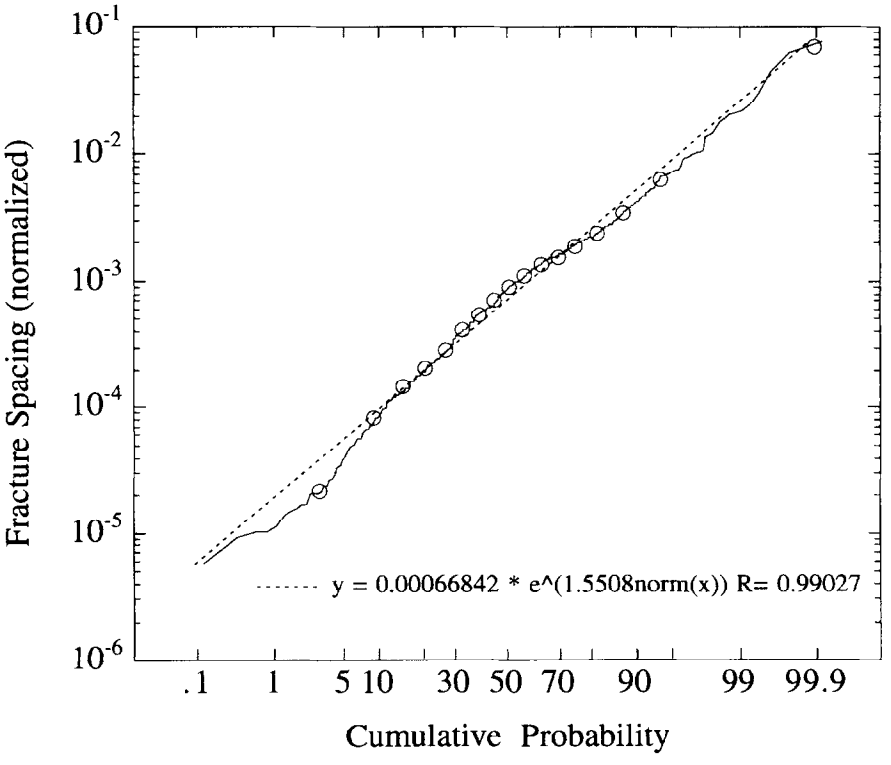

Fig. 11. Results of fracture spacing from simulation using the heterogeneous cascade and plotted as cumulative probability. Here the data could be interpreted as being log-normal. This is especially true for the largest 30% of the values. When plotted as log–log cumulative frequency (Fig. 6) these data appear to have a power-law slope. This seeming contradiction can be understood by recognising the large standard deviation indicated by the regression.

power-law distributions (Montroll and Schlesinger, 1982).

Figure 11 is a cumulative probability plot of fracture spacing using the results from the fracture simulation with the heterogeneous cascade (Fig. 6). On these axes, a log-normal distribution will plot as a straight line. Deviation from a linear relationship is not large and it would not be unreasonable to call this 'log-normal' especially for the large values that when plotted as log size vs log cumulative frequency constitute the power-law tail with a slope of 1.2 (Fig. 6).

Several explanations are possible for spacing distributions interpreted to be log-normal. These include: (a) the data appear log-normal for the majority of the sample other than a small number of values (tails) that depart from log-normality (Fig. 1); (b) the data can be log-normal, but with a large dispersion that makes the larger values appear 'power-law' when plotted as cumulative frequency on log–log coordinates (Fig. 6); (c) the data can be log-normal with small dispersion. In all cases the relationship can be fit by modifying parameters of Lévy-stable distributions. It also demonstrates that when viewed in terms of Lévy-stable distributions, log-normal and fractal distributions are not distinct, but part of a continuum being defined by different Lévy parameters.

DISCUSSION

Studies of power-law joint or fault attributes measured at different scales have raised questions about how to relate deformation at varying scales and incorporate resolution dependency (Peacock and Sanderson, 1994; Peacock, 1996). The strain-based multiplicative cascade approach advocated here answers these questions with certain limitations. Resolution dependency is addressed through the number of faults or fractures simulated, with larger numbers being indicative of improved resolution. It is a necessary alternative to better known fractal simulation techniques of reservoir properties (Hewett, 1986; Painter *et al.*, 1995) where information is available at a very small scale from well logs. Using this latter approach, the scaling character of a reservoir parameter (e.g. porosity) is interpolated using a single statistical moment (usually variance). Unlike porosity, however, only small numbers of faults or fractures are measured from either seismic or outcrop and extrapolation to smaller scales is necessary. This extrapolation is made using the multiplicative cascade technique with the assumption that the random multipliers come from a single Lévy-stable distribution. Use of this assumption means that the resulting cascade measures are self-similar.

Examples of attributes measured at different scales show similar log cumulative frequency vs log size slopes (fractal dimensions) in some cases (Castaing *et al.*, 1996; Odling, 1997), but variation in dimension in others (Yielding *et al.*, 1996; Nicol *et al.*, 1996). Understanding these differences is necessary to obtain some level of confidence in the ability to extrapolate to smaller scales. Preliminary suggestions (Yielding *et al.*, 1992) were that (log–log) extrapolation to core-scale could be done directly from the seismic data, however, further study has found this not to be the case (Yielding *et al.*, 1996).

Extrapolation of an attribute scaling distribution is usually done by extending the power-law relationship to smaller size values. This projected distribution, however, is for *the entire area* covered by the attribute distribution. Furthermore, belief that the same fractal dimension will exist in a subarea implies that the attribute is self-similar. A less restrictive model is for the fractal dimensions defined by log–log cumulative frequency relationship to vary spatially, meaning that the attribute is self-affine. If a large area with a given log–log slope is divided into smaller areas, each subarea can have a fractal dimension that differs both from that of the large area and other subareas (Belfield, 1992). Averaging of the fractal dimensions in all of the subareas seems to yield the value for the extended slope. The additive nature of Lévy-stable distributions is such that by creating a union all of the attribute data in the subareas (even if the subareas have Lévy distributions with different dimensions) in a single plot will result in a fractal dimension equivalent to that of the extended slope. This observation implies that prediction of an attribute distribution at a smaller scale requires an understanding of the spatial characteristics of the scaling structure.

With the self-similar cascade process used here, resultant spacing distribution will be approximately the same at all scales. This restrictive criteria can be moderated by choosing random multipliers from different (Lévy-stable) distributions. The result will be a self-affine spacing distribution that varies with scale. Still problematical in this endeavour is the range of scale (levels of cascade) that the strain measures can be considered self-similar and when do they become self-affine. Answers to this question may lie in studying multiple reduced scale subareas from extensive data sets (Castaing *et al.*, 1996; Watterson, *et al.*, 1996; Odling, 1997).

CONCLUSIONS

Numerous examples indicate that faults and fractures follow some type of geometrical self-organisation and are not distributed randomly in space. This requires non-Poissonian techniques to spatially distribute stochastic faults and fractures in realistic geometries. One approach is to use a strain distribution model as a spatial guide or template for the simulation. In this model, strain is multifractal and generated via a multiplicative cascade. This insures a scale-invariant structure of the resulting fracture or fault geometry. Random values for the cascade come from Lévy-stable distributions, the parameters of which determine the (self-similar) characteristics of the strain distribution. Lévy distributions are also shown to fit attribute distribution functions and are used to sample aperture sizes in the stochastic modelling.

Spacing distribution functions ranging from approximately exponential to power-law depend on the spatial partitioning of strain. Simulation of stochastic fractures on a homogeneously distributed strain measure template leads to approximate exponential spacing distribution, but a power-law spacing distribution is found by using a heterogeneous strain measure. When plotting spacing as log–log cumulative frequency, the slope (fractal dimension) quantifies the degree of clustering. Small fractal dimensions are indicative of more clustering than large ones, the degree of clustering decreasing with an increase in fractal dimension. In this sense an estimate of fractal dimension of fracture spacing based on core, outcrop, or well log data provides a better characterisation of spatial distribution than does other statistics such as average spacing.

Acknowledgements—I would like to thank G. Jones, Q. Fisher and R. Knipe for the opportunity to present a preliminary version of this work at the Faulting, Fault Sealing and Fluid Flow in Hydrocarbon Reservoirs conference at Leeds University, UK, in September 1996. S. Painter kindly provided the program for the Lévy random number generator. Discussions with J. Muller, A. Saucier and T. Rives were helpful. T. Engelder and J. Watterson are thanked for their reviews that helped improve the manuscript. This work was supported, in part, by Gas Research Institute through contract GRI ⌗5093-220-2826. Approval of ARCO management for publication of this paper is appreciated.

REFERENCES

Barton, C. C. (1995) Fractal analysis of scaling and spatial clustering of fractures. In *Fractals in the Earth Sciences*, ed. C. C. Barton and P. R. LaPointe, pp. 141–178. Plenum Press, New York.

Barton, C. C. and Larson, E. (1985) Fractal geometry of two-dimensional fracture networks at Yucca Mountain, southwestern Nevada. In *Proceedings of the International Symposium on Fundamentals of Rock Joints*, ed. O. Stephannson, pp. 77–84, Bjorkliden, Sweden.

Becker, A. and Gross, M. R. (1996) Mechanism for joint saturation in mechanically layered rocks: an example from southern Israel. *Tectonophysics* **257**, 223–237.

Belfield, W. C. (1992) Simulation of subseismic faults using fractal and multifractal geometry, (paper SPE 24751). *Proceedings of the SPE Annual Technical Conference*, 903–911.

Belfield, W. C. (1994) Multifractal characteristics of natural fracture apertures. *Geophysical Research Letters* **21**, 2641–2644.

Belfield, W. C. and Sovich, J. (1995) Fracture statistics from horizontal wellbores. *Journal of Canadian Petroleum Technology* **34**, 47–50.

Brooks, B. A., Allmendinger, R. W. and de la Barra, Garrido I. (1996) Fault spacing in the El Teniente Mine, central Chile: evidence for nonfractal fault geometry. *Journal of Geophysical Research* **101**, 13633–13653.

Cacas, M. C., de Marsily, G., Tillie, B., Barbeau, A., Durand, E., Feuga, B. and Peaudecerf, P. (1990) Modeling fracture flow with a stochastic discrete fracture network: calibration and validation I. The flow model. *Water Resources Research* **26,** 479–489.

Castaing, C., Halawani, M. A., Gervais, F., Chilès, J. P., Genter, A., Bourgine, B., Ouillon, G., Brosse, J. M., Martin, P., Genna, A., Janjou, D. (1996) Scaling relationships in intraplate fracture systems related to Red Sea rifting. *Tectonophysics* **261,** 291–314.

Childs, C., Walsh, J. J. and Watterson, J. (1990) A method for estimation of the density of fault displacements below the limits of seismic resolution in reservoir formations. In *North Sea Oil and Gas Reservoirs II*, ed. A. T. Buller, E. Berg, O. Hjelmeland, J. Kleppe, O. Torsaeter and J. O. Aasen, pp. 309–318. Graham & Trotman, London.

Chilès, J. P. (1988) Fractal and geostatistical methods for modeling of a fracture network. *Mathematical Geology* **20,** 631–654.

Chilès, J. P. and de Marsily, G. (1993) Stochastic models of fracture systems and their use in flow and transport modeling. In *Flow and Contaminant Transport in Fractured Rock*, ed. J. Bear, C. F. Tsang and G. de Marsily, pp. 169–231. Academic Press, San Diego.

Cowie, P. A., Sornette, D. and Vanneste, C. (1995) Multifractal scaling properties of a growing fault population. *Geophysical Journal International* **122,** 457–469.

Davis, A., Marshak, A., Wiscombe, W. and Cahalan, R. (1994) Multifractal characterizations of nonstationarity and intermittency in geophysical fields: observed, retrieved, or simulated. *Journal of Geophysical Research* **99,** 8055–8072.

Einstein, H. H. and Baecher, G. B. (1983) Probabilistic and statistical methods in engineering geology specific methods and examples. *Rock Mechanics and Rock Engineering* **16,** 39–72.

Evertsz, C. J. G. and Mandelbrot, B. B. (1992) Multifractal measures. In *Chaos and Fractals*, ed. H. O. Peitgen, H. Jurgens and D. Saupe, pp. 921–953. Springer, Berlin.

Feller, W. (1971) *An Introduction to Probability Theory and Its Applications*. J. Wiley & Sons, New York, Vol. II, p. 669.

Gauthier, B. D. M. and Lake, S. D. (1993) Probabilistic modeling of faults below the limit of seismic resolution in the Pelican Field, North Sea, offshore U.K. *Bulletin of the American Association of Petroleum Geologists* **77,** 761–777.

Gillespie, P. A., Howard, C. B., Walsh, J. J. and Watterson, J. (1993) Measurement and characterisation of spatial distribution of fractures. *Tectonophysics* **226,** 113–141.

Godderij, R. R. G. G., Chessa, A. G., Bruining, J. and Kreft, E. (1995) Conditional simulation of subseismic faults (paper SPE 30620). *Proceedings of the SPE Annual Technical Conference*, 939–951.

Gross, M. R. and Engelder, T. (1995) Strain accommodated by brittle failure in adjacent units of the Monterey Formation, U.S.A.: scale effects and evidence for uniform displacement boundary conditions. *Journal of Structural Geology* **17,** 1303–1318.

Heffer, K. J. and Bevan, T. G. (1990) Scaling relationships in natural fractures—data, theory, and applications (paper SPE 20981). *Proceedings of the Europoean Petrology Conference* **2,** 367–376.

Hestir, K., Chiles, J. P., Long, J. and Billaux, D. (1987) Three dimensional modeling of fractures in rock: from data to a regionalized parent–daughter model. In *Flow and Transport Through Unsaturated Fractured Rock*, ed. D. D. Evans and T. J. Nicholson. Geophysical Monograph, 42, pp. 133–140. American Geophysical Union, Washington, DC.

Hewett, T. A. (1986) Fractal distributions of reservoir heterogeneity and their influence on fluid transport (paper SPE 15386). *Proceedings of the SPE Annual Technical Conference*, 843–850.

Jackson, P. and Sanderson, D. J. (1992) Scaling of fault displacements from the Badajoz Cordoba shear zone, SW Spain. *Tectonophysics* **210,** 179–190.

Knott, S. D., Beach, A., Brockbank, P. J., Brown, J. L., McCallum, J. E. and Welbon, A. I. (1996) Spatial and mechanical controls on normal fault populations. *Journal of Structural Geology* **18,** 359–372.

Laubach, S. E. (1991) Fracture patterns in low-permeability gas reservoir rocks in the Rocky Mountain region. (paper SPE 21853). *Proceedings of the SPE Rocky Mountain Low-Permeability Reservoir Symposium*, pp. 501–510.

Long, J. C. S., Remer, J. S., Wilson, C. R. and Witherspoon, P. A. (1982) Porous media equivalents for networks of discontinuous fractures. *Water Resources Research* **18,** 645–658.

Long, J. C. S. and Billaux, D. M. (1987) From field data to fracture network modeling: an example incorporating spatial structure. *Water Resources Research* **23,** 1201–1216.

Main, I. (1996) Statistical physics, seismogenesis, and seismic hazard. *Reviews of Geophysics* **34,** 433–462.

Mandelbrot, B. B. (1982) *The Fractal Geometry of Nature*. W.H. Freeman, New York.

Mantegna, R. N. (1994) Fast, accurate algorithm for numerical simulation of Lévy-stable stochastic processes. *Physical Review (E)* **49,** 4677–4683.

Mantegna, R. N. and Stanley, H. E. (1995) Scaling behaviour in the dynamics of an economic index. *Nature* **376,** 46–49.

Marrett, R. and Allmendinger, R. (1991) Estimates of strain due to brittle faulting: sampling of fault populations. *Journal of Structural Geology* **13,** 735–738.

Montroll, E. W. and Shlesinger, M. F. (1982) On 1/f noise and other distributions with long tails. *Proceedings of the National Academy of Sciences* **79,** 3380–3383.

Munthe, K. L., Orme, H., Holden, L., Damsleth, E., Heffer, K., Olsen, T. S. and Watterson, J. (1993) Subseimic faults in reservior description and simulation (paper SPE 26500). *Proceedings of the SPE Annual Technical Conference*, 843–850.

Narr, W. and Suppe, J. (1991) Joint spacing in sedimentary rocks. *Journal of Structural Geology* **13,** 1037–1048.

Nicol, A., Walsh, J. J., Watterson, J. and Gillespie, P. A. (1996) Fault size distributions–are they really power-law. *Journal of Structural Geology* **18,** 191–197.

Odling, N. E. (1992) Network properties of a two-dimensional fracture pattern. *Pure and Applied Geophysics* **138,** 95–114.

Odling, N. E. (1997) Scaling and connectivity of joint systems in sandstones from western Norway. *Journal of Structural Geology* **19,** 1257–1271.

Painter, S., Paterson, L. and Boult, P. (1995) Improved technique for the stochastic interpolation of reservoir properties (paper SPE 30599). *Proceedings of the SPE Annual Technical Conference*, 750–745.

Peacock, D. C. P. (1996) Field examples of variations in fault patterns at different scales. *Terra Nova* **8,** 361–371.

Peacock, D. C. P. and Sanderson, D. J. (1994) Strain and scaling of faults in the Chalk at Flambrough Head, U.K. *Journal of Structural Geology* **16,** 97–107.

Pollard, D. D. and Segall, P. (1987) Theoretical displacements and stresses near fractures in rock: with applications to faults, joints, veins, dikes, and solution surfaces. In *Fracture Mechanics of Rocks*, pp. 277–349, ed. B. K. Atkinson. Academic Press, London.

Rives, T., Razack, M., Petit, J-P. and Rawnsley, K. D. (1992) Joint spacing: analogue and numerical simulations. *Journal of Structural Geology* **14,** 925–937.

Schlische, R. W., Young, S. S., Ackermann, R. V. and Gupta, A. (1996) Geometry and scaling relations of a population of very small rift-related normal faults. *Geology* **24,** 683–686.

Tchalenko, J. S. (1970) Similarities between shear zones of different magnitudes. *Bulletin of the Geological Society of America* **81,** 1625–1640.

Walsh, J. J. and Watterson, J. (1993) Fractal analysis of fracture patterns using the standard box-counting technique: valid and invalid methodologies. *Journal of Structural Geology* **15,** 1509–1512.

Watterson, J., Walsh, J. J., Gillespie, P. A. and Easton, S. (1996) Scaling systematics of fault sizes on a large-scale range fault map. *Journal of Structural Geology* **18,** 199–214.

Wu, H., Willemse, E. J. M. and Pollard, D. (1995) Prediction of fracture density and drainage distance in layered rock masses using borehole data. In *Proceedings of Eurorock '94: Rock Mechanics in Petroleum Engineering*, pp. 487–494, Delft, The Netherlands.

Yielding, G., Walsh, J. J. and Watterson, J. (1992) The prediction of small-scale faulting in reservoirs. *First Break* **10,** 449–460.

Yielding, G., Needham, T. and Jones, H. (1996) Sampling of fault populations using sub-surface data: A Review. *Journal of Structural Geology* **18,** 135–146.